Structural, electronic and optical properties of chromium carbide (Cr₃C) as potential counter electrode material: a first principle study

Abdulkareem Hussaini[1], Alhassan Shuaibu[1]*, Isaac Daniel Hyuk[1], Abdullahi Lawal[2], Ismail Magaji[1] and Rabi Mustapha[3]

[1]Department of Physics, Faculty of Science, Kaduna State University, P.M.B 2339, Kaduna State, Nigeria.
[2]Department of Physics, Federal College of Education, P.M.B 1041 Zaria, Kaduna State, Nigeria.
[3]Department of Computer Science, Faculty of Science, Kaduna State University, P.M.B 2339, Kaduna State, Nigeria.

Correspondence: alhassan.shuaibu@kasu.edu.ng

Abstract

Transition metal carbides are recently considered to be potential substitutes to platinum counter electrode due to their low cost, high catalytic activity and good thermal stability. In this paper, we investigate the structural, electronics, and optical properties of one of the transition metal carbides (Cr₃C). The structural and electronic properties were computed using the first principles approach, a generalized gradient approximation (PBE-GGA) as exchange correlation functional within density functional theory (DFT) was used for the calculations. The optimized lattice parameters of the compound were $a = 4.525$ Å, $b = 5.186$ Å, $c = 6.659$ Å and $\propto = \beta = \gamma = 90.0^0$ which are in agreement with number of theoretical and experimental results. The calculated band gap and density of state (DOS) of this compound reveals the presence of Valence Band Maximum (VBM) and Conduction Band Minimum (CBM) at different symmetry point with the intersection of several energy bands crossing the Fermi level, this interaction indicate a metallicity nature and may cost the conductive nature of the material to have sufficient electro-catalytic ability for the reduction of I₃⁻ ions in counter electrode of DSSCs. The optical properties are calculated from the spectra of dielectric function alongside with the other related optical properties like energy loss function, reflectivity, refractive index, extinction coefficient and conductivity within a continuous energy range of 0 to 16eV. The obtained results of the optical properties of this material show that the materials can be use as possible candidates for counter electrode of DSSC.

1.0 Introduction

Dye-sensitized solar cells (DSSCs) are third-generations photovoltaic devices with mesoporous architecture and some attractive features, such as cost effectiveness, environment friendliness, easy processing, and relatively high-power conversion efficiency (PCE). Guo *et al.* (2015). Over the past few decades, DSSCs have been intensively studied to improve the photovoltaic performance and reduce production cost. Kay and Gratzel, (1996). Among the basic components of DSSCs is the counter-electrode (CE), which has two important roles: to collect electrons from the external circuit; and to transfer the electrons to recycle the redox species of the redox couple (I³/I) through catalytic reduction. Thus, the nature of CE is important in determining the photovoltaic performance of DSSCs. Superior CE catalysts possess high electro catalytic activity, good electrical conductivity, and chemical stability. Papageorgiou, (2004). Based on these standards, platinum is a noble metal that has been widely used to fabricate efficient CEs for DSSCs. Although, the high

cost, limited resources, and corrosion by iodine species in electrolyte solution seriously restricts the large-scale application of Pt-based CEs in DSSCs. Guo *et al.* (2015). Therefore, economic, stable, and effective non-Pt catalysts should be exploited to fabricate novel CEs.

All transition metal (Ti, Zr, Hf, Ta, Nb, V, Cr, Mo, W, Fe, Co, Ni, etc.) compounds (TMCs), such as oxides, nitrides, carbides, sulphides, selenides, tellurides and phosphides, conducting polymers, carbon materials (mesoporous carbon, activated carbon, carbon black, conductive carbon, carbon dyes, carbon fibers, carbon nanotubes, fullerene and graphene), metals and alloys (Fe, Co, Ni, Pt, etc.), and their corresponding hybrids have been tested and developed as CE materials in DSSCs (Yun *et al.,* 2014; Wu and Ma, 2014; Thomas *et al.,* 2014). However, these CE materials face many challenges. Catalytic activity is an intrinsic characteristic of a catalyst, which is determined by the electronic structure of the catalyst. Thus, the catalytic mechanism of these materials (TMCs, conducting polymers and carbon materials) as CE catalysts in DSSCs is not clear even though they exhibit superior catalytic activity (Kim *et al.,* 2018). In this case, predicting which CE materials will exhibit superior catalytic activity in DSSCs is exceedingly difficult (Wu *et al.,* 2017). To overcome these challenges, the first-principle DFT calculations and the ab initio investigation, combined with advanced techniques, such as XRD, SEM, TEM, photovoltaic tests, and electrochemical tests, should be employed. Using these combinations would elucidate the relationship between the electronic structure and the catalytic activity of CE materials and reveal the transport properties of electrons and ions at the electrolyte/CE interface from the macro to atomic level, which is critical in establishing the catalytic mechanism of CE materials in DSSCs (Zhang *et al.,* 2017).

Finally, the structural design and functional modification of CE catalytic materials can be realized at atomic and molecular levels based on the relationship between the electronic structure and the catalytic activity, and between thechargetransportandtheinterfaceproperties.Elucidati ngthecatalyticmechanismwillprovidethe theoretical guidance andtechnicalsupporttocommercializeCEcatalyticmate rials,therebypromoting the rapid development of new solar cells (Yun *et al.,* 2014; Wu and Ma, 2014; Thomas *et al.,* 2014).

In this work, we study the structural, electronics and optical properties of Cr_3C within the frame work of Density Functional Theory (DFT) and Density Functional Perturbation Theory as implemented in quantum espresso (GE).

2.0 Computational details

Geometric relaxation and electronic properties of Cr_3C were performed by first principles approach based on plane-wave self-consistent field (PWSCF) program within the frame work of DFT as implemented in quantum-espresso simulation package. Giannozzi, *et al.* (2009).

The simulation adopted the super cell in orthorhombic phase Cr_3C with 16 ions, with 12 Chromium atoms and 4 Carbon atoms respectively. The core electrons were optimized by norm-conserving pseudo potentials of the standard solid-state pseudo potential library to model the interaction between valence electron and ionic core potential for Cr, and C. A generalized gradient approximation (GGA) functional of Perdew – Berke-Erzndof (PBE) as exchange correlation function is usedin order to treat electron-electron interaction. Pardew, Burke, Ernzerhof, (1996). The monkhorste-pack scheme k-points grid sampling was set as $6 \times 10 \times 6$ for the irreducible Brillouin zone was used. 400eV was chosen as kinetic energy cutoff. The initial structure obtained from materials project. Jain, *et al.* (2013). were geometrically relaxed for atomic coordinates and dimension of the cell using intrinsic Broyden– Fletcher – Goldfarb – Shanno (BFGS) algorithm. Onida, Reining, and Rubio, (2002). Until atomic maximum forces were less than 5×10^{-5}eV and total energy during iterative process was changing by less than 0.0001Ry. The optical properties were calculated using real and imaginary parts of the dielectric tensor. It is well known that the main optical parameters of the crystal are related by their complex dielectric function;

$$\varepsilon(\omega) = \varepsilon_1(\omega) + i\varepsilon_2(\omega) \qquad (1)$$

Where $\varepsilon_1(\omega)$ the real is part and $\varepsilon_2(\omega)$ is the imaginary part of the dielectric function.

The real and imaginary part of the dielectric function have been calculated using the linear response within the Density Functional Perturbation theory (DFPT) as implemented in Quantum ESPRESSO based on equation 2 and 3. Kootstra, De Boeij, and Snijders, (2000).

$$(2)$$

$$\varepsilon_1(\omega) = 1 + \frac{2}{\pi} \int_0^\infty \frac{\varepsilon_2(\omega)\omega' d\omega'}{\omega'^2 - \omega^2}$$

$$\varepsilon_2(\omega) = \frac{Ve^2}{2\pi m^2 \omega^2} x \int d^3k \sum_{nm'} |kn|p|kn'|^2 f(kn) x [1 - f(kn')] \partial(E_{kn} - E_{kn'} - \omega) \tag{3}$$

Where p is the momentum matrix element between states of n and $n!$ the fermi distribution function is given by $f(kn)$. While the crystal wave function is $|kn|$ and corresponding nth eigen value is E_{kn}.

The knowledge of electron loss function, real and imaginary parts of frequency dependent dielectric function expressions was used to compute other optical parameters namely; absorption index $\alpha(\omega)$, refractive index $n(\omega)$, extinction index $k(\omega)$, conductivity $\sigma(\omega)$, and reflectivity $R(\omega)$ as shown in the following equations (Abdullahi and Shaari, 2017).

$$\alpha(\omega) = \frac{\omega}{c} \sqrt{2(\varepsilon_1^2(\omega) + \varepsilon_2^2(\omega))} - \epsilon_1(\omega) \tag{4}$$

$$n(\omega) = \sqrt{\left(\frac{\varepsilon_1(\omega) + \sqrt{\varepsilon_1^2(\omega) + \varepsilon_2^2}}{2}\right)} \tag{5}$$

$$k(\omega) = \sqrt{\frac{-\varepsilon_1(\omega) + \sqrt{\varepsilon_1^2(\omega) + \varepsilon_2^2}}{2}} \tag{6}$$

$$\sigma(\omega) = \frac{\omega \epsilon_2(\omega)}{4\pi} \tag{7}$$

$$R(\omega) = \left|\frac{\sqrt{\epsilon(\omega)} - 1}{\sqrt{\epsilon(\omega)} + 1}\right|^2 \tag{8}$$

3.0 Result and discussion
3.1 Structural properties

The space group *Pnma [62]* and point group *mmm* which is an orthorhombic crystal structure and the lattice constants are $a = 4.525$ Å, $b = 5.186$ Å, $c = 6.659$ Å and $\propto = \beta = \gamma = 90.0^0$. The calculation adopts a super cell orthorhombic phase Cr_3C containing sixteen atoms; twelve chromium atom and four carbon atoms respectively. The norm – conserving pseudo potentials are chosen for the calculation; result is more consistent the experimental results than ultra-soft pseudo potentials. Venkatraman, and Neumann, (1990); Ganguly, Murthy, and Kannoorpatti, (2020). The relaxed unit cell of pure orthorhombic phase Cr_3C is shown in Figure 1.
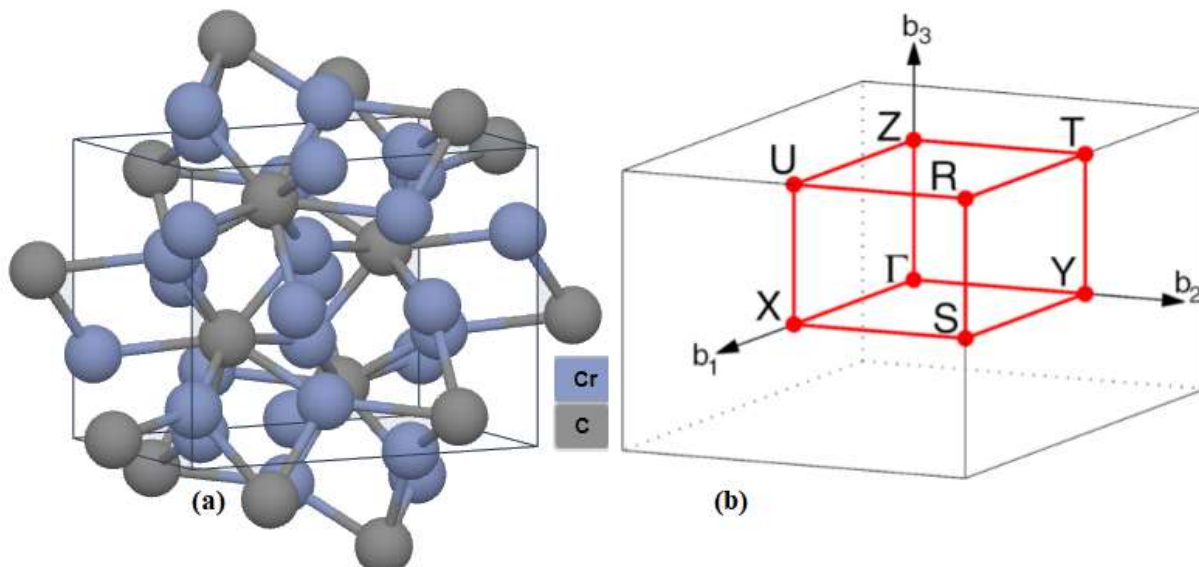

Figure 1: Optimized 2×2×2 supercell crystal of Cr₃C, (b) the Brilliun zone for symmetry of band structure calculation

95

3.2 Electronic properties

Electronic band structure and density of states (DOS) calculation is very important for describing the optoelectronic behavior of materials. Here we perform an analysis of band structure, DOS and partial density of state (PDOS) of Cr_3C. The electronic band structures of Cr_3C were computed within PBE approximation based on DFT along special symmetry directions of the irreducible Brillion zone setting fermi level scale at 0eV represented by dotted line as can be seen in Figure 2(a) and (b) respectively. The bands were selected along 16 symmetry points, their energy range of band structure is plotted from -10.00eV to 10.00eV, the compound reveals the presence of valence band maximum (VBM) and conduction band minimum (CBM) at different symmetry point, (at point Z and U) indicating that the compound is more up metallic in nature. This is because the Fermi level intersecting several energy bands within the top of VBM and CBM, this may lead the conductive nature of this compound to have sufficient electro-catalytic ability for the reduction of I_3^- ions in counter electrode of DSSCs, this result in line with what was reported in Papageorgiou, (2004). The partial density of state (PDOS) shown in Figure 2(c), indicate that there are anti bonding states of s-p at fermi level (0eV), showing s-p is involved in the electrical conduction process of Cr_3C indicating the possibility of both covalent and ionic bonding in Cr_3C.
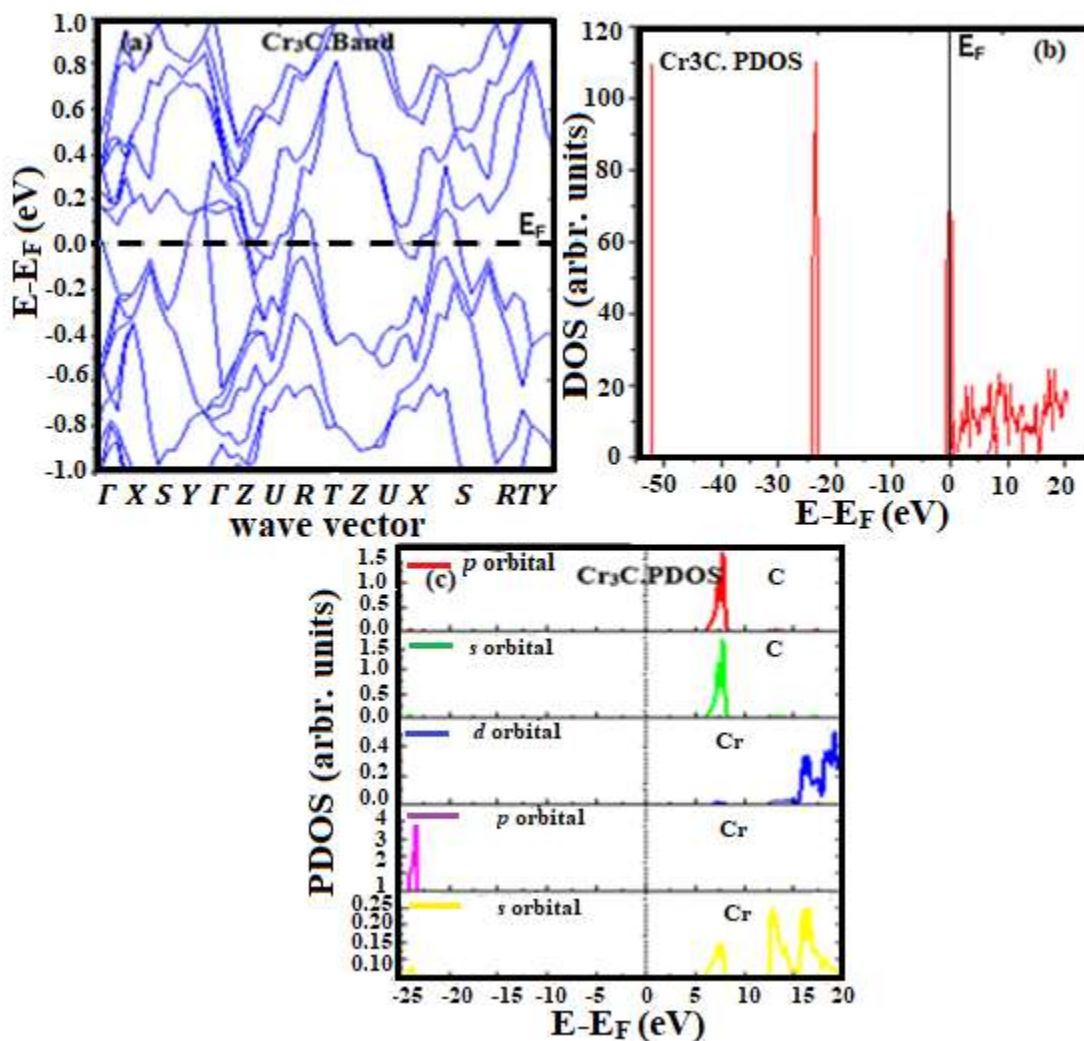

Figure 2 (a) Calculated Band structure, (b) corresponding Density of state and (c) Partial Density of State of Cr_3C within the DFT-GGA

3.3 Optical properties

Investigating the optical properties of materials plays a vital role in understanding their optoelectronic applications. We have calculated the optical properties of the material by evaluating the microscopic dielectric function via time dependent density

functional theory (TDDFT). The first microscopic dielectric function describes the behavior of linear response of a material to the electromagnetic radiation field applied which displays the absorptive character of the material. Yabana *et al.* (2012). Real part of the dielectric describes how much material polarized as a result of induced electric dipole creation when electric field is applied; while imaginary part indicates how much material absorb photon energy. From equation 1, 2 and equation 3, it is clearly seen that $\varepsilon_1(\omega)$ can be obtained using imaginary part, $\varepsilon_2(\omega)$. The dielectric functions for the material consist of three components $\varepsilon_{xx}, \varepsilon_{yy}, \varepsilon_{zz}$ which are related to the polarizations along *x, y, z* directions. Figure 3(a), present the imaginary part of the dielectric function of Cr$_3$C, we noticed the presence of prominent peaks at z-z direction. Interestingly, the compound can absorb photon energy up to 9.092eV as the imaginary line approaches zero. The relatively strong absorption in 0.304 – 9.092eV energy range provides strong evidence that the compound has the potential to be used for detecting light within broadband range. The dielectric constant of the compound at high frequency along perpendicular $\varepsilon(\infty)$ direction was found to be 100.00. In both cases, these results indicate that the material could have a greater performance of the excellent efficiency in light harvesting for DSSC

(Malik *et al.,* 2020). Figure 3(b) presents the real part of the dielectric function of Cr$_3$C, we noticed the presence of prominent peaks at z-z direction, and the prominent peak is at -150.00. The negative character of the real part indicates that the incident photons are totally reflecting in these regions for the material. These results are in agreement with some theoretical results of similar compound (Bagci *et al.,* 2016).

Electron energy loss function is used in describing the loss in energy of a fast-moving electron traversing the material. Figure 3(c), present the electron energy loss function of Cr$_3$C, the prominent peak was found to be 14.243eV. The sharp maxima peak of the energy loss function spectra indicates the existence of plasma resonance and this appear at a particular incident light frequency which correspond to the trailing edges in the reflection spectra sometimes called plasma frequency. At this point of energy, the imaginary part of the dielectric function goes to zero indicating rapid reduction in reflectance. Figure 3(d), represent the absorption index of the title material, it is observed that the absorption spectrum begins from 0.607eV and rises sharply until attaining maximum peak at 9.73 x 10^{-5}cm^{-1} which correspond to 0.910eV, and then decreases down to 14.85eV which reveal the broadband wavelengths absorption behavior of the compound. This compound shows good absorption coefficient in the region from 1.516eV to 11.819eV.
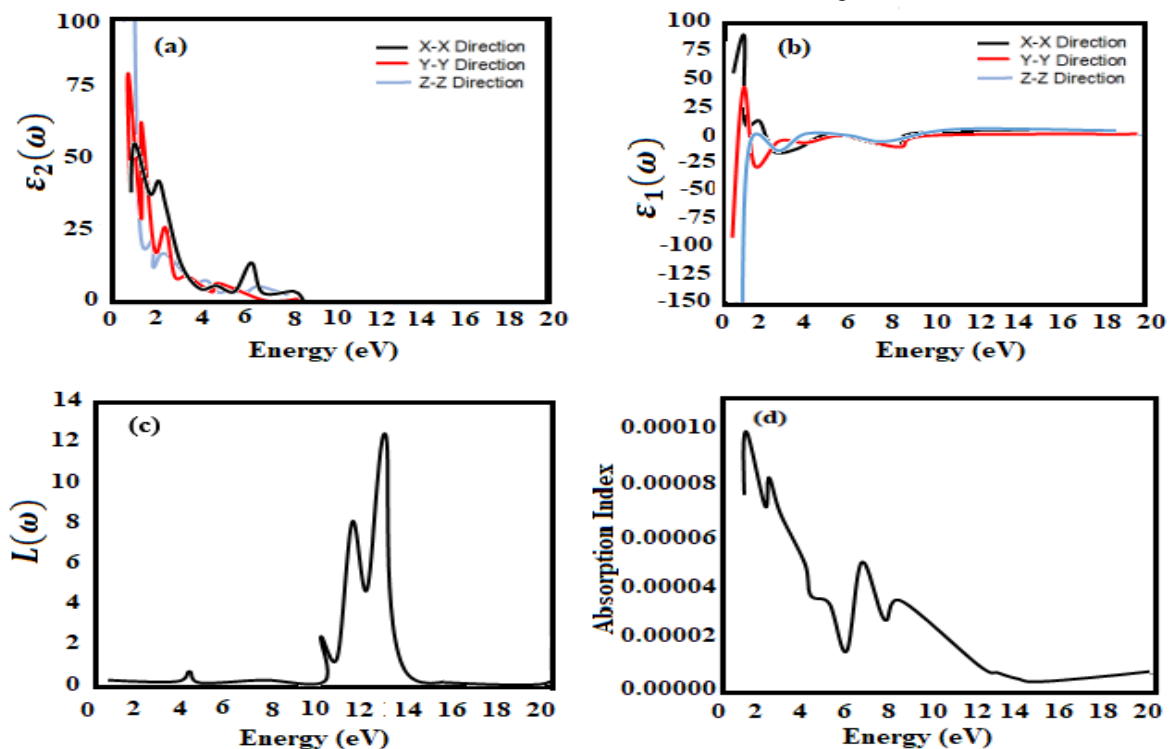

Figure 3: (a) Imaginary part of the dielectric function of Cr$_3$C, (b) Real part of the dielectric function of Cr$_3$C, (c) Energy Loss function of Cr$_3$C, (d) Absorption Index of Cr$_3$C

As one of the optical property parameters, the refractive index is a quantity that describes how much light is refracted after entering the material. Abdullahi Lawal; A. Shaari, R. A. N. J. (2017). Figure 4 (a) and (b) shows the refractive index and extinction index of Cr_3C as a function of energy. The refractive index and

extinction index were both found to be 5.1448. From the refractive and extinction index graph, we notice that the compound possesses high refractive index within visible region around and decreases at higher energy in ultraviolet region.
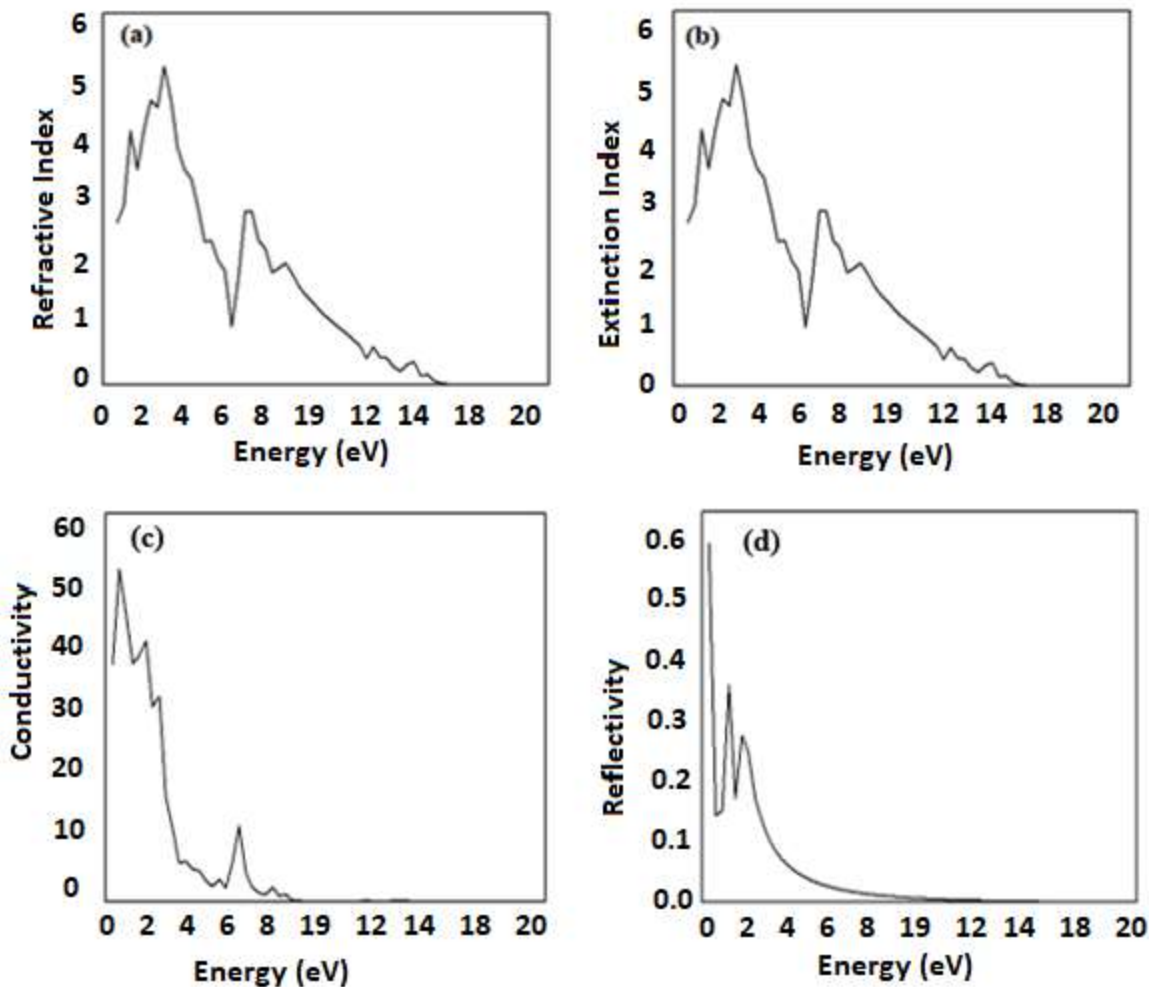

Figure 4: (a) Refractive Index of Cr_3C, (b)Extinction Index of Cr_3C,(c)Conductivity of Cr_3C, and (d)Reflectivity of Cr_3C

A complex conductivity spectrum is a measure of photoconductivity that gives clear information on the electrical conductivity of a material. Figure 4 (c) shows the complex conductivity spectrum as a function of photon energy. It is shown that the maximum peak is located at 0.91eV corresponding to $55.651S^{-1}$, indicating high conductance at low energy. Therefore, Cr_3C is more conductive in the incident photon energy range from 0.910eV to 8.183eV.
Reflectivity is the change in reflected photon energy from the surface to the photon energy incident on the surface. Figure 4 (d) present the changes in reflectivity spectrum with photon energy; the reflectivity spectrum

starts to increase from about 15% until it reaches maximum level of 36.15% corresponding to photon energy value of 0.607eV and decreases drastically to a very low value. Indicating that the material is transmitting in visible wavelengths because of small reflectance within that energy range.

4.0 Conclusion
In summary, we have performed a comprehensive first principles study of the structural, electronics and optical properties of the transition metal carbides (Cr_3C). Our calculated lattice parameters are found to be in excellent agreement with experiments and some

98

theoretical results. For the electronic structure calculations, our band structure results indicate the material is metallic in nature with possible high conductivity and the PDOS shows that the chemical bonding in Cr$_3$C has a complex mixture of metallic, covalent, and ionic characters. While for the optical responses, we observed that the main peaks in the imaginary part of dielectric are due to electronic transitions from Cr-s, Cr-p, C-s, C-p. The variations in ϵ_2 (ω) along *x, y, z* varies with the possible nature of band structure of the material i.e., shows an opposite semiconducting nature. Our material reflects the possible strong optical absorption in both visible and ultra violet regions and is suitable for replacing Pt as Counter electrode in DSSC applications. The present study is believed to serve as a useful reference for the fabrication of this novel material for applications.

Declarations

Ethics approval and consent to participate

Not Applicable

Consent for publication

All authors have read and consented to the submission of the manuscript.

Availability of data and material

Not Applicable.

Competing interests

All authors declare no competing interests.

Funding

There was no funding for the current report.

References

Abdullahi Lawal; A. Shaari, R. A. N. J. (2017). *Sb2Te3 crystal a potential absorber material for broadband photodetector_ A first-principles study _ Elsevier Enhanced Reader.pdf* (pp. 2302–2310). pp. 2302–2310. Results in Physics.

Ab Malik Marwan, N. A., Md Jahangir Alam, N. N., Samat, M. H., Mohyedin, M. Z., Hussain, N. H., Hassan, O. H., ... and Mohamad Taib, M. F. (2020). First-principles studies on structural, electronic and optical properties of Fe-doped NiS2 counter electrode for Dye-sensitized solar cells using DFT+ U. *Scientific Research Journal*, *17*(2), 82-98.

Bagci, S., Yalcin, B. G., Aliabad, H. R., Duman, S., and Salmankurt, B. A. H. A. D. I. R. (2016). Structural, electronic, optical, vibrational and transport properties of CuBX 2 (X= S, Se, Te) chalcopyrites. *RSC advances*, *6*(64), 59527-59540.

Ganguly, A., Murthy, V., and Kannoorpatti, K. (2020). Structural and electronic properties of chromium carbides and Fe-substituted chromium carbides. *Materials Research Express*, *7*(5), 056508.

Giannozzi, P., Baroni, S., Bonini, N., Calandra, M., Car, R., Cavazzoni, C., Dabo, I. (2009). QUANTUM ESPRESSO: a modular and open-source software project for quantum simulations of materials. Journal of physics: Condensed Matter, 21 (39), 395502.

Guo, J., Liang, S., Shi, Y., Hao, C., Wang, X., and Ma, T. (2015). Transition metal selenides as efficient counter-electrode materials for dye-sensitized solar cells. *Physical Chemistry Chemical Physics*, *17*(43), 28985-28992.

Jain, A., Ong, S. P., Hautier, G., Chen, W., Richards, W. D., Dacek, S., Cholia, S., Gunter, D., Skinner, D., Ceder, G., and Persson, K. A. (2013). The material project: A materials

Kay, A., and Grätzel, M. (1996). Low cost photovoltaic modules based on dye sensitized nanocrystalline titanium dioxide and carbon powder. *Solar Energy Materials and Solar Cells*, *44*(1), 99-117.

Kim, J. S., Kim, B., Kim, H., and Kang, K. (2018). Recent progress on multimetal oxide catalysts for the oxygen evolution reaction. *Advanced Energy Materials*, *8*(11), 1702774.

Kootstra, F., De Boeij, P. L., and Snijders, J. G. (2000). Application of time-dependent density-functional theory to the dielectric function of various nonmetallic crystals. *Physical Review B*, *62*(11), 7071.

Onida G, Reining L, Rubio A. Electronic excitations: density – functional versus many – body Greens – function approaches. Rev Mod Phys 2002; 74:601

Papageorgiou, N. (2004). Counter-electrode function in nano crystalline photo electrochemical cell configurations. *Coordination Chemistry Reviews*, *248*(13-14), 1421-1446.

Pardew JP, Burke K, Ernzerhof M. Generalized gradient approximation made simple. Phys Rev Lett 1996:77:3865.

Stewart JJ. MOPAC: a semiempirical molecular orbital program, J Compu Aided Mol Des 1990;4:1 – 103

Venkatraman, M., and Neumann, J. P. (1990). The C-Cr (carbon-chromium) system. *Bulletin of Alloy Phase Diagrams*, *11*(2), 152-159.

Wu, J., Lan, Z., Lin, J., Huang, M., Huang, Y., Fan, L., ... and Wei, Y. (2017). Counter electrodes in dye-sensitized solar cells. *Chemical Society Reviews*, *46*(19), 5975-6023.

Wu, M., and Ma, T. (2014). Recent progress of counter electrode catalysts in dye-sensitized solar cells.*The Journal of Physical Chemistry C*, *118*(30), 16727-16742.

Yabana, K., Sugiyama, T., Shinohara, Y., Otobe, T., and Bertsch, G. F. (2012). Time-dependent density functional theory for strong

electromagnetic fields in crystalline solids. *Physical Review B*, *85*(4), 045134.

Yun, S., Hagfeldt, A., and Ma, T. (2014). Pt-free counter electrode for dye-sensitized solar cells with high efficiency. *Advanced Materials*, *26*(36), 6210-6237.

Zhang, T., Yun, S., Li, X., Huang, X., Hou, Y., Liu, Y., ... and Fang, W. (2017). Fabrication of niobium-based oxides/oxynitrides/nitrides and their applications in dye-sensitized solar cells and anaerobic digestion. *Journal of Power Sources*, *340*, 325-336.